ELSEVIER

Journal of Power Sources 114 (2003) 309–319

JOURNAL OF POWER SOURCES

www.elsevier.com/locate/jpowsour

Techniques to improve the usability of nickel–hydrogen cells

L.H. Thaller*, A.H. Zimmerman, G.A. To

The Aerospace Corporation, El Segundo, CA 90245, USA

Received 18 September 2002; accepted 26 September 2002

Abstract

The voltages at which the different charging and discharging peaks occur in a nickel electrode were investigated for a set of six representative electrodes. The impact of cycling temperature, electrolyte concentration, and cycling history on these different electrodes resulted in alterations in the usable capacities of the electrodes and/or the efficiency of the charging reaction. The cobalt level in the active material, the KOH concentration of the electrolyte, and the cycling temperature were all found to impact the position of the charging peaks of the beta and the gamma charging reactions. The position of the oxygen evolution characteristic was found to be mainly a function of the cycling temperature. The findings of these studies resulted in recommendations for selecting certain cell design factors and charging protocols that will lead to improved cycle lives and higher levels of usable cell capacities.

Keywords: Nickel electrodes; Charging characteristics; Cycle life

1. Background

Nickel–hydrogen cells and batteries have reached a high level of maturity in terms of their use in both geosynchronous and low Earth orbit (LEO) satellite applications. There have been several suppliers of these cells and batteries to the aerospace industry. Over the years, different preferences have developed related to the concentration of potassium hydroxide used as the electrolyte and the percentage of cobalt additive incorporated into the lattice of the nickel hydroxide that serves as the active material in the nickel electrode. The cycling temperature and the recharge protocol have also been the object of much discussion. No uniform consensus exists for the different factors that are available to the power system design engineer. Following an extensive review of the NASA-funded and Air Force-funded LEO data basing programs carried out on this cell chemistry [1] coupled with in-house research studies into the functioning of the active material used in the nickel electrode [2–4], the reasons for some of these differences in design and operating preferences have become evident. The information from this earlier review has been augmented with more recent laboratory studies to help clarify several factors that impact the functioning of nickel electrodes. These findings have been organized in a manner that a potential power system designer can more clearly understand the pros and cons that are associated with the different design choices and cycling conditions that are available to him.

2. Introduction

When planning for a mission using nickel–hydrogen batteries, there can be several different overall objectives. One might be to maximize the usable energy density of the battery over the required mission life. This requires that the capacity walkdown [5] that is typically experienced during extended cycling, be held to within acceptable values. Another objective might be to optimize the cycling efficiency in order to minimize the amount of solar array needed during the recharge portion of the cycle. The requirement here is to minimize the amount of overcharge while at the same time maintaining the minimum state-of-charge above a certain value. Still another objective might be to maximize the cycle life of the battery. This requires cycling conditions that minimize the rates of the different capacity loss mechanisms that are known to occur in nickel–hydrogen cells during long-term cycling, while still maintaining the required amount of usable capacity [3]. To optimize the conditions to meet these three different objectives will require different selections related to the cobalt content of

* Corresponding author. Tel.: +1-310-336-6180; fax: +1-310-336-5846.
E-mail address: lawrence.h.thaller@aero.org (L.H. Thaller).

0378-7753/03/$ – see front matter
PII: S0378-7753(02)00534-7

the nickel-hydroxide active material, the potassium hydroxide (KOH) concentration of the electrolyte, the cycling temperature, and the details of the charging protocol. Beyond these factors, which are selected based on beginning-of-life considerations, the changes and the rates of these changes in the charging requirements as the batteries are cycled under the conditions selected at the beginning of the mission must be understood as well.

To approach these questions in a more formalized method, several areas must be researched and documented in detail. The first area concerns the impact the cell design factors and cycling conditions have on the position of the charging peaks for the beta-phase material, the gamma phase material, and the voltage where oxygen evolution represents a significant parallel reaction during the charging process. It is necessary to know how these potentials change (1) as the cobalt content of the active material is changed [5,6], (2) as the KOH concentration of the electrolyte is changed [7,8], and (3) as the cycling temperature is changed [9]. The potentials at which these reactions occur will also change slightly as the electrodes are cycled due to the naturally occurring degradation mechanisms within the nickel electrodes. Once this information is in hand, the charge efficiencies as impacted by the cell cycling conditions and the changes caused by the cycling conditions must be determined. One final factor that must be considered is the impact of different cycling conditions on the ultimate cycle life of the cell or battery. This report addresses these three different areas separately.

3. Position of the charging peaks and oxygen evolution character

In this report, the term ‘‘cell design’’ will not include factors such as number of plates, cell diameter, or type of plaque material. It will be assumed that a cell design is being considered that has already displayed satisfactory cycling results over 40,000–60,000 LEO cycles in previous tests. Cell design will be limited to selections of the KOH concentration of the electrolyte and cobalt levels used in the active material. The cycling temperature will be another major variable that will be included in this section since the position of the beta and gamma charging peaks as well as the oxygen evolution characteristics will be impacted by this variable.

3.1. Experimental techniques

Many of the results to be reported here were obtained using the electrochemical voltage spectroscopy (EVS) technique that has been described earlier [10]. Another standard technique used in our laboratory determines the capacity of sample pieces of electrode when cycled using several charge/discharge sequences. This flooded utilization (FU) test first cycles the electrode sample to the beta phase and then to the gamma phase during the next cycling sequence. Both of these techniques utilize samples (approx. 1.0 cm^2) taken from a 3.5- or 4.5-in. diameter electrode. References to studies carried out within other organizations related to the characteristics of the nickel electrode are included. Where possible, the cycling history of individual pressure vessel (IPV) nickel–hydrogen cells will be presented where they support the results stemming from laboratory studies carried out here or in other laboratories.

3.2. Major information available from an EVS scan

Fig. 1 is a composite of two different EVS scans. They were generated by very slowly charging and discharging a sample of nickel electrode material [10]. Voltage is measured relative to a mercury/mercuric oxide reference electrode. By adding about 1.0 V to these numbers, the voltage relative to a hydrogen electrode would be obtained. In this plot, the charging part of the scan is shown in the portion below zero, and the discharging portion of the scan appears in the positive portion of the plot. For illustrative purposes, the charging portion of the scan was from one electrode and the discharge portion of the scan was taken from a different electrode.

This figure may be understood as follows. It is well established that during the charging of nickel electrodes from a fully discharged condition, the active material is first charged to the beta phase as the average valence of the nickel changes from +2 to +3 [8]. Following this, some of the material can be charged to the gamma phase where the average valence of the nickel is +3.66. This second process often occurs in parallel with the evolution of oxygen at the nickel electrode. To increase the usable energy density of the nickel electrode and at the same time to minimize the damage to the electrode and increase the charge efficiency of the charging step, there should be as wide a separation as possible between the potential at which the active material is charged to the gamma phase and the potential at which large amounts of oxygen are evolved. However, at the cycling temperatures in common use, these latter two reactions generally occur in parallel at about the same potential.

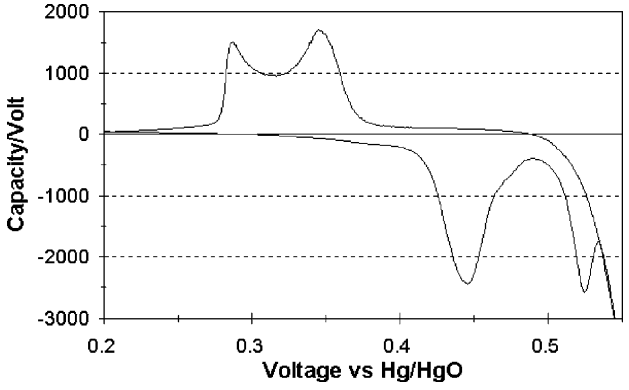

Fig. 1. Major charging and discharge features available from an EVS scan.

Table 1
Description of the electrodes used in the EVS and FU studies

Plate no.	Number of cycles	Approximately percentage of Co	Cycling temperature (°C)	Electrode concentration (percentage of KOH)	Recharge ratio (%)
1	20	5	+20	31	Varied
2	40,000	5	+10	26	104
3	40,000	5	−5	26	103
4	40,000	10	+10	31	104
5	Not cycled	5	N.A.	N.A.	N.A.
6	Not cycled	10	N.A.	N.A.	N.A.

In the example shown in Fig. 1, the broad peak that occurs between about 0.41 V and extending to about 0.49 V is where the discharged active material is charged to the beta form of the active material. The next higher peak, which extends from about 0.50 to about 0.53 V, is where the charged active material is charged further to the gamma phase. The line to the right of the gamma charging peak is where the current involved with the formation of oxygen increases logarithmically with potential. During the discharge portion of the cycle, the material that is in the beta phase will discharge first since the voltage at which it discharges is higher than the voltage at which the gamma phase material discharges. The peaks for these processes occur at about 0.35 V for the discharge of the beta material and 0.27 V for the discharge of the gamma phase material. The relative amounts of beta and gamma material depend on the recharge ratio, end-of-charge voltage, and cycling temperature employed during the charging step. When electrode material is cycled at temperatures and charging rates usually seen in actual cell cycling, the gamma charging peak moves to the right and is often seen only as a shoulder on the oxygen evolution curve.

The exact position of these peaks, especially the charging peaks, is a function of the cobalt content of the active material, the KOH concentration used in the electrolyte, the cycling temperature, and the amount of corrosion that has taken place thus far during the cycling. These relationships are understood in principle, but the following sections will help quantify them based on our laboratory studies and a review of supporting studies carried out elsewhere. By more firmly establishing the location of these peaks as a function of the above-listed variables, issues related to the pros and cons of selecting different cobalt levels, electrolyte KOH concentrations, and cycling temperatures can be examined more accurately.

3.3. Experimental program

Six different electrodes formed the major focus of this study. They had experienced different amounts of LEO cycling, different cycling temperatures, etc. as listed in Table 1. The objective was to select production-grade electrodes that came from different backgrounds and had different cycling histories. They were all viewed to be free of any manufacturing problems. All of these electrodes were submitted to EVS as well as FU cycling tests. Other EVS scans used in this study were from our earlier studies [3,10].

It is seen that some of the electrodes were never assembled into cells while others have successfully cycled to about 40,000 LEO cycles before they were taken off test. Different cobalt levels, KOH concentrations, recharge ratios, and cycling temperatures were also represented in this group.

3.3.1. EVS cycling studies

EVS cycling [10] was conducted at room temperature and at −5 °C as part of the investigation of the influence of temperature on the position of the different peaks depicted in Fig. 1. A computer was used to drive the source meter that was incorporated into the EVS apparatus. The program set into the computer first discharged any remaining charged material by lowering the voltage by 2 μV/s until the voltage versus the mercury/mercuric oxide (Hg/HgO) reference electrode was 0.20 V. The pre-selected voltage was then increased at the rate of 2 μV/s until the end-of-charge voltage was reached. For the samples tested at room temperature, the cut-off voltage was 0.53 V, and at −5 °C it was 0.56 V. At these voltages, all of the discharge took place close to 0.27 V, indicating that all of the material had been charged to the gamma phase. Tables 2 and 3 summarize the information gathered during the second complete EVS cycle. The information gathered during the first or condi-

Table 2
Summary of room-temperature EVS Scans

Plate no.	Beta peak (V)	Gamma peak (V)	Oxygen position[a] (V)	Gamma–beta[b] (V)	Gamma discharge (V)
1	0.452	None	0.505	N.A.	0.277
2	0.457	0.51	0.505	0.053	0.277
3	0.450	None	0.505	N.A.	0.276
4	0.456	0.51	0.505	0.054	0.276
5	0.450	None	0.485	0.060	0.272
6	0.408	None	0.505	N.A.	0.262

[a] The term oxygen position is the voltage at which the rate of oxygen evolution is significant relative to the conversion of active material to the gamma phase. The selected rate of oxygen evolution was equal in all cases.

[b] The value is the difference in the peak voltages for charging to the beta phase and charging to the gamma phase.

Table 3
Summary of −5 °C EVS scans

Plate no.	Beta peak (V)	Gamma peak (V)	Oxygen level[a] (V)	Gamma–beta[b] (V)	Gamma discharge (V)
1	0.451	0.532	0.545	0.081	0.278
2	0.450	0.527	0.550	0.077	0.279
3	0.442	0.530	0.550	0.088	0.276
4	0.445	0.525	0.540	0.080	0.278
5	0.442	0.528	0.545	0.086	0.279
6	0.412	None	0.550	N.A.	0.269

[a] The term oxygen position is the voltage at which the rate of oxygen evolution is significant relative to the conversion of active material to the gamma phase. The selected rate of oxygen evolution was equal in all cases.
[b] The value is the difference in the peak voltages for charging to the beta phase and charging to the gamma phase.

tioning cycle will be discussed in a later section that will address the cycling characteristics of material that has remained in either the charged state or the discharged state for extended periods of time.

In viewing the EVS summary tables, several items are evident. At both test temperatures, plate no. 6 is significantly different from the others in terms of the position of the two charging peaks and the discharging peak. By having the beta charging peak located 30–40 mV lower than the other plate samples, the charging processes will occur further away from the potentials at which significant amounts of oxygen are evolved. The well-cycled plate, no. 4, which also had cobalt content of about 10% when manufactured, no longer shows any difference from the plate samples that were manufactured with cobalt contents closer to 5%. There was no consistent movement of the position of the beta charging peaks due to changes in temperature. The gamma peaks shifted to a significantly higher voltage at the lower temperature, but the oxygen evolution character shifted even more than the gamma peaks at the lower temperature. The absence of a distinct gamma peak at the higher temperature for some of the plate samples was indicative of the gamma peaks being positioned at or about the same potential as the oxygen evolution line. The positions of the gamma peak at room temperature, where they are listed, appeared only as shoulders on the oxygen evolution line.

The exact position of these peaks, especially the charging peaks, are a function of the cobalt content of the active material, the KOH concentration used in the electrolyte, the cycling temperature, and the amount of corrosion that has taken place during the cycling. These functions are now understood in principle and can be described in words as follows.

1. *The beta charging peak*: The position of this peak is a function of a number of factors. An important one is related to the half-cell potential as impacted by KOH concentration (the higher the concentration, the lower the half-cell voltage) [7,8], the cobalt content in the active material (the higher the cobalt content the lower the half-cell voltage) [5,6], and the cycling temperature (the higher the temperature, the lower the half-cell voltage) [9]. The position of this peak will move to higher voltages as the electrode is cycled since there will be a build-up of non-cobalt-containing corrosion products adjacent to the nickel sinter current collector. The kinetic factors along with the half-cell voltages combine to establish the shape and the position of this and other peaks, as they would appear on an EVS scan.
2. *The gamma charging peak*: The position of the gamma charging peak from a theoretical point of view should appear at a lower potential than the beta charging peak since the gamma material is thermodynamically more stable than the beta-phase material. In fact, the active material that is not continuously charged and discharged will slowly convert to charged gamma phase material over the course of many charge/discharge cycles. From extended EVS studies, the gamma peak always appears at a significantly higher voltage than the beta charge peak. Data suggest that the span between these two peaks at −5 °C is between 80 and 90 mV, while at +25 °C, the span is closer to 50 mV.
3. *The oxygen evolution reaction*: This reaction does not have a peak since the reaction involves the electrolysis of an almost infinite supply of water. Oxygen evolution is an extremely irreversible reaction that thermodynamics would suggest should occur at voltages well below both the theoretical position of the gamma as well as the beta charging peak. There is some evidence that when cobalt is added to the active material, not only do the charging reactions take place at lower voltages, but the oxygen evolution occurs at a slightly higher voltage [5]. As the temperature is lowered, the kinetics of this highly irreversible reaction are reduced even further, and the voltage at which significant amounts of oxygen are evolved is moved to a higher voltage. At −5 °C, the voltage for oxygen evolution occurs about 50 mV higher than at room temperature. This facilitates the separation between the gamma charging peak and prevents the onset of excessive amounts of oxygen evolution. The overall result will be higher charge efficiency, a higher usable energy density when cycling at colder temperatures, and a smaller amount of oxygen evolution. This results in less damage to the nickel electrode during cycling and less waste heat due to the catalytic combination of the evolved oxygen with hydrogen.
4. *The position of the beta discharge peak*: This peak can be completely absent depending on how much of the active material has been charged to the gamma phase. Where some of the material is still in the beta phase, its discharge peak will discharge at a voltage that depends on the beta charging peak. There is evidence that at lower temperatures, the discharge peak will move to slightly lower voltages.
5. *The position of the gamma discharge peak*: This peak will depend on the temperature and cobalt content of the

Table 4
Summary of −5 °C FU cycling

Plate no.	First 10-h capacity (mAh)	Second 10-h capacity (mAh)	14-h Capacity (mAh)	Gain (%) to cycle 3[a]	Gain (walk down) at −5 °C[b]
1	30.45	31.89	41.14	29.01	4.55
2	24.75	29.22	36.44	24.71	22.32
3	26.94	28.05	35.91	28.02	15.98
4	25.77	27.92	39.15	40.22	23.70
5	28.99	30.25	36.69	21.29	12.00
6	30.81	31.74	38.55	21.46	9.02

[a] The percentage gain to cycle 3 is the increase in capacity at the 10 mA rate over that obtained at the 10 mA rate following the second 10 h charge.
[b] The percentage gain at −5 °C is the gain at the 10 mA rate at cycle 3 versus the capacity at the 10 mA rate at cycle 3 obtained at room temperature.

active material. It is not known how the position of the discharge peak will depend on the KOH concentration. Based on the data contained in Tables 4 and 5, little difference was seen in the position of the gamma discharge peaks at the two temperatures that were examined.

The above statements are based on the assumption that the electrodes have been cycled for one or two cycles prior to making these measurements. In the case of active material that has not been cycled for several weeks, the beta and gamma charge peaks will move to higher voltages depending on the temperature, the cobalt content of the active material, and most likely the KOH concentration of the electrolyte. From testing of different samples of electrode material, the maximum in the beta charging peak and the gamma–gamma both move to higher voltages. In the case of room temperature EVS studies, this temporary shift is between 20 and 30 mV, while at −5 °C, the extent of this shift to higher voltages is between 40 and 60 mV. This shift makes it more difficult to charge electrodes that have been left in the discharged state for an extended period of time. Based on the one case that has been studied, active material that has been left in the charged state for an extended period of time will move to a lower voltage during discharge. Reference [8] listed the reversible potential for the "activated" and "deactivated" forms of the beta and gamma materials.

From these statements, the following situations can be more easily understood.

1. Larger amounts of usable capacity are available when cycling is carried out at lower temperatures since the kinetics of the oxygen evolution reaction are reduced, causing the onset of oxygen evolution to occur at higher voltages. This allows a larger percentage of the beta material to be charged to the gamma state prior to the onset of excessive amounts of oxygen evolution. Fig. 2 shows this very clearly. In this figure, the EVS scans for two samples taken from the same electrode are shown. One was scanned at room temperature, and other was scanned at −5 °C. The oxygen evolution curve has moved about 50 mV to the right, allowing the charging to the gamma phase of some of the active material.

Table 5
Summary of room temperature FU cycling

Plate no.	First 10-h capacity (mAh)	Second 10-h capacity (mAh)	14-h Capacity (mAh)	Gain (%) to cycle 3[a]
1	30.88	32.54	39.39	20.93
2	25.32	24.91	29.79	19.59
3	26.94	28.91	30.96	7.09
4	24.88	27.84	31.65	13.69
5	28.76	28.89	32.76	13.40
6	29.08	30.61	35.36	15.52

[a] The percentage gain to cycle 3 is the increase in capacity at the 10-mA rate over that obtained at the 10-mA rate following the second 10-h charge.

2. Larger amounts of capacity walkdown will occur in cells filled with 26% KOH compared with 31% KOH because the reversible half-cell voltage of the nickel electrode is higher in 26% KOH cell by 10–20 mV. Capacity walkdown is a term used to describe the temporary loss of usable capacity over the first few thousand LEO cycles caused by a slightly lower charge efficiency that

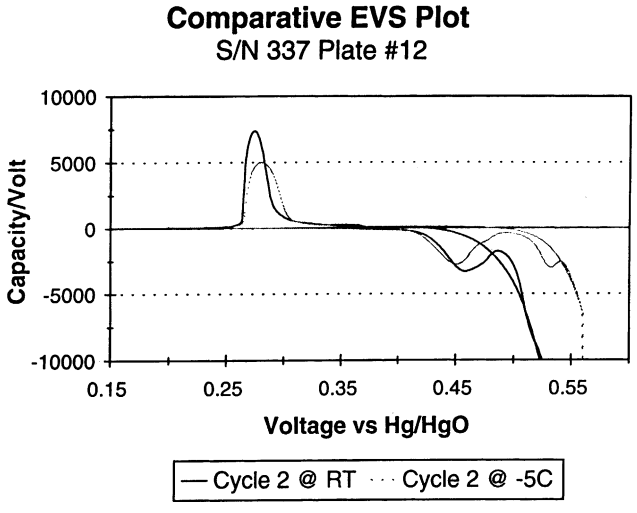

Fig. 2. EVS scans of samples from the same electrode tested at two different temperatures.

results from the gamma charging peak being a few millivolts closer to the where significant amounts of oxygen are evolved. This causes more of the charging to take place in parallel with oxygen evolution. The remedy for this is to lower the cycling temperature. This will reduce the amount of oxygen evolution by reducing the kinetics (exchange current) for that reaction.

3. As electrode corrosion occurs over the cycling history of a cell, there is a gradual build-up of non-cobalt-containing active material adjacent to the nickel sinter current collector. A reduction in the cobalt content of the active material increases the voltage needed to charge the electrode. In so doing, there will be a larger amount of oxygen evolved during the charging process. This will result in a gradual reduction in the charging efficiency of the electrode accompanied by a gradual reduction in the state-of-charge of the cell. This is another cause for capacity walkdown during extended cycling. The remedy for this problem is to lower the cycling temperature. This will reduce the amount of oxygen evolution by reducing the kinetics (exchange current) for that reaction.
4. Increased cobalt content in the active material results in a lower charging voltage for these electrodes. The reversible potential of electrodes as well as the charging peaks move further away from the potentials at which oxygen is evolved. This increases the separation between the reactions that result in charging the active material and the reaction resulting in the evolution of oxygen. There is also evidence that the addition of cobalt to the active material increases the overpotential for oxygen evolution [5]. By reducing the exchange current of the oxygen evolution reaction, the separation in voltage between the charging reaction and the oxygen evolution reaction is increased even further.
5. Active material that is not being charged or discharged will slowly convert to a structural form that changes the voltage at which it is charged or discharged [3]. This has been attributed to Ostwald ripening, although crystallographic studies have not confirmed these changes. In the case of discharged material at room temperature, a higher voltage by 20–30 mV must be used to charge this modified form of active material (40–60 mV at −5 °C). In the case of charged material that has converted to its modified form, a discharge voltage at room temperature that is lower by about 20 mV is experienced during its subsequent discharge. To increase the chargeability of this material, it is suggested to reduce the cycling temperature to reduce the amount of co-evolution of oxygen gas. When attempting to recharge material that has reverted to the form that is more difficult to recharge, it is important to be able to use an end-of-charge voltage above a threshold value needed to bring about the transition to the form of the active material that charges at a lower voltage [3].

3.3.2. Flooded utilization (FU) studies

The FU testing was also carried out on all six samples of electrode material at both −5 and 20 °C. As in the EVS testing, the samples were about 1.0 cm^2 in area. They were cut from the same electrode as the samples used for the EVS testing. In the FU testing, the samples were charged and discharged at rates that were more representative of actual use in a nickel–hydrogen cell. The first cycle was used to convert the nickel hydroxide from an inactive form to the active form seen when an electrode is repeatedly cycled. The second cycle charges the electrode at about the *C*/10 rate for 10 h to convert the nickel hydroxide mostly to the beta phase of nickel oxyhydroxide. The capacity available at the 10, 2, and 0.1 mA discharge rates are then determined with the help of a computer-controlled discharge sequence and data collection system.

Following this, a third cycle is used to convert a significant portion of the charged material to the gamma phase. A charge rate of about *C*/10 for 14 h is used (40% overcharge). Again the discharge capacities at the 10, 2, and, 0.1 mA rates are determined. Fig. 3 displays a typical FU plot obtained for the case of plate no. 3 at −5 °C. Pertinent aspects of the results of these experiments are tabulated in Tables 6 and 4 using the same identifiers as noted in Table 1.

The information contained in both these tables illustrates the significant amount of capacity that is gained charging for longer periods of time and/or charging at lower temperatures. There is a significant trend suggesting that electrodes that have been cycled for extended periods of time display larger amounts of capacity gain when charged at the lower temperature. Well-cycled cells incur larger amounts of plaque corrosion, particularly when cycled at higher temperatures. This non-cobalt-containing form of active material will be seen in Section 3.3.4 to have a higher charging voltage than the cobalt-containing active material. Plate sample no. 3 was cycled at −5 °C during its extended cycling test and behaves closer to the electrodes that have not been cycled.

3.3.3. Cell cycling data

Life cycle testing of 10-cell packs tested at the Navy facility at Crane, IN under Air Force sponsorship provided supporting information relative to the usable capacity of

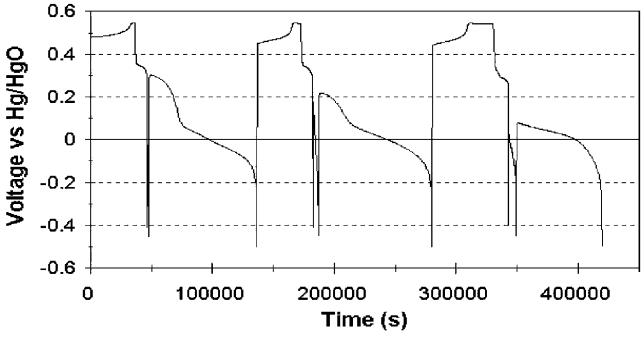

Fig. 3. Flooded Utilization results for plate no. 3 at −5 °C.

Table 6
Comparison of cell capacities following about 40,000 LEO cycles

Step no.	Discharge step	Charge step	Cells cycled at +10 °C	Cell cycled at −5 °C
1		As cycled in test	1.04 RR (41.60 Ah)	1.03 RR (41.2 Ah)
2	*C* rate to 1.0 V		21.7 Ah	46.8 Ah
3	*C*/10 rate to 1.0 V		11.3 Ah	7.7 Ah
4	Total first discharge		33.0 Ah	54.5 Ah
5		*C*/2 rate	48.9 Ah	48.9 Ah
6		*C*/10 rate	14.8 Ah	14.9 Ah
7		Total charge	63.7 Ah	63.8 Ah
8	*C* rate		49.9 Ah	50.2 Ah
9	*C*/10 rate		7.7 Ah	9.0 Ah
10	Total second discharge		57.6 Ah	59.2 Ah

cells of like design that were cycled at different temperatures, one cell pack at +10 °C and the other at −5 °C. Table 6 appeared in an earlier report [3] and contains the usable capacity that was available from one cell from each pack that was removed from testing prior to cell failure. The plate nos. 2 and 3 used in the EVS and FU tests were taken from the cells whose capacity characteristics are tabulated in Table 6.

In this side-by-side comparison of a cycling test carried out at +10 °C and another at −5 °C, the results are very revealing. The staff at the Navy facility at Crane, IN generated this data. The cells were first discharged following a normal discharge that was part of the cycling test at the *C* rate and then the *C*/10 rate to 1.0 V so the remaining cell capacity could be measured. Then they were recharged in a manner that included a significant amount of overcharge. Then the discharge was repeated. From the information continued in Table 6 it can be concluded that the cells that were cycling at +10 °C were cycling between lower states-of-charge than the cells that were cycling at −5 °C.

3.3.4. Literature sources

Studies by others have investigated the impact of several important variables on the positions of the different charging peaks. A figure in the 1993 NASA nickel–hydrogen handbook [7] contains a summary of the results that varied the KOH concentration used in the cells and determined the average discharge voltage and the cell capacities that resulted from these changes. These findings appear as Fig. 4.

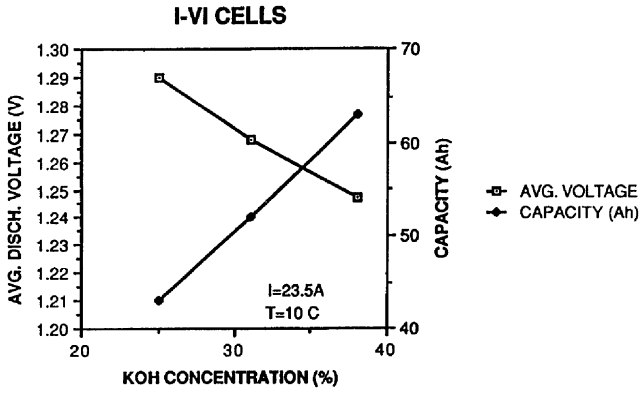

Fig. 4. Changes in discharge voltage and capacity as a function of electrolyte concentration.

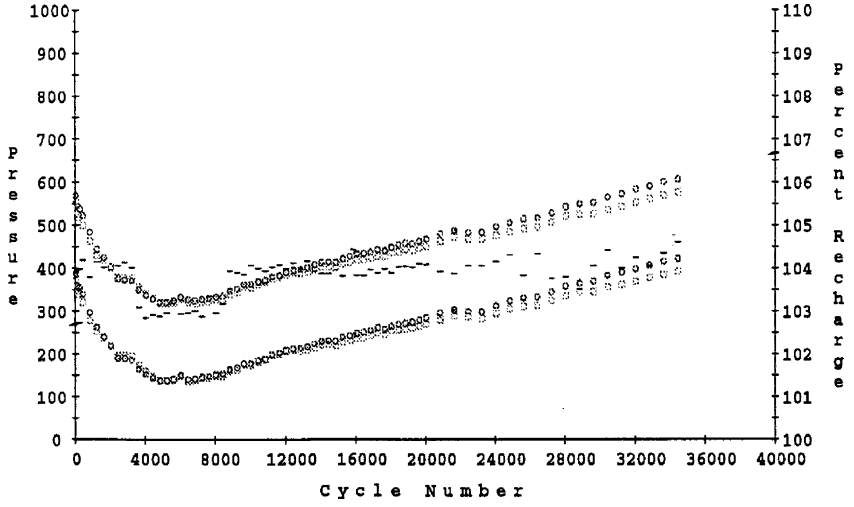

Fig. 5. Source of information used to make estimates of peak pressures and amounts of capacity walkdown.

The data contained in Fig. 4 indicate that as the electrolyte concentration is raised to higher levels of KOH, the useable capacity of the cells will be higher, and the average discharge voltage of the cells will be lower by a few millivolts. For this reason, the cells for the Intelsat program in its early stages at least were filled with KOH solutions that were about 36% KOH. When other NASA-sponsored studies found that lower KOH concentrations resulted in the longer cycle lives [11] required of LEO applications, it was found that, as expected, they had slightly higher operating voltages and lower usable ampere hours capacities. Another aspect that was found to be undesirable by some users was the tendency to experience larger amounts of capacity walkdown as illustrated in Fig. 5. The capacity loss, as suggested by the drop in end-of-charge pressure over the first few thousand cycling, is referred to as capacity walkdown.

Table 7 is a collection of information taken from a group of side-by-side tests carried out under sponsorship by NASA and the Air Force. By reviewing the data, the amounts of capacity walkdown in terms of percentage of the nameplate capacity that was lost due to the cycling conditions selected for the test are determined and listed in the table. These estimates were based in the reduction in the end-of-charge pressures.

No similar information is available for cells cycled at −5 °C or 60% DOD since cells cycled under these conditions tend not to walkdown from their original starting capacities as estimated from the end-of-charge pressure [3]. Based on these side-by-side comparisons, there is a consistent trend for the cells activated with 26% KOH to walkdown in capacity to a greater degree than the cell activated with 31% KOH. Based on our newer understanding of the beginning-of-life capacity as a function of KOH concentration, it is felt that if the information related to tests 2-a and 2-b were reversed in terms of their KOH concentration, it would be more consistent with the other five sets of information.

Table 7
Percentage capacity walkdown as a function of electrolyte concentration for cells cycled at +10 °C

Pack no.	Electrode concentration (percentage of KOH)	Maximum BOL pressure (psi)	Walkdown (%)
1-a	31	606	33
1-b	26	567	42
2-a	31	605	31
2-b	26	685	20
3-a	31	725	31
3-b	26	680	43
4-a	31	787	14
4-b	26	700	23
5-a	31	795	11
5-b	26	697	35
6-a	31	705	16
6-b	26	660	29

The information in Fig. 6 [5] shows that higher cobalt concentrations in the active material not only results in a lower charging voltage, but an oxygen evolution characteristic that occurs at a higher voltage. Both of these factors contribute to the feature shown on the right hand side of the Fig. 4 indicating that more capacity can be charged into the electrode due to the wider separation between the voltage at which the electrode is charged and the voltage at which oxygen is evolved.

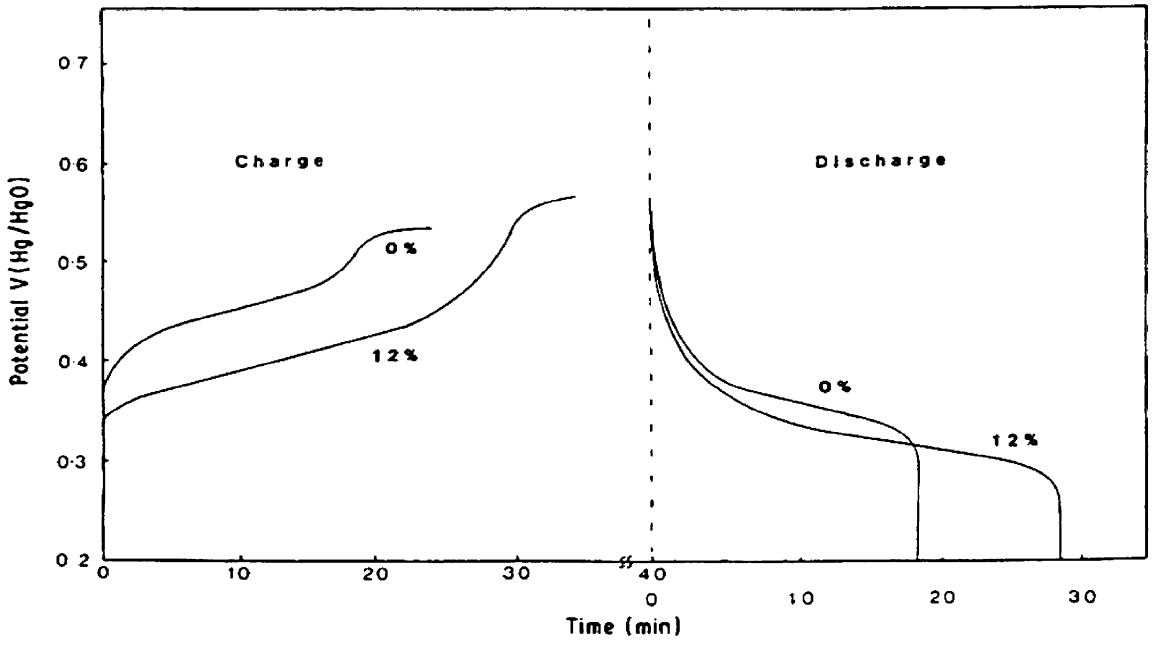

Fig. 6. Changes in charging potential and oxygen evolution characteristics as a function of cobalt content of the active material at room temperature.

4. Impact of cycling conditions and cell design features on cycling efficiency

In Section 3 of this report, the impact of the cell design variables was measured by the capacity of the different electrodes. In this section, the main factor to be considered will be the impact on the cycling efficiency and how that is impacted by cycling temperature. Since the ampere hours efficiency over a complete charge/discharge cycle depends on the significance of the oxygen evolution characteristics of the electrode under test, it should vary according to where the different charging potentials are positioned on a figure similar to Fig. 1. When spacecraft are being designed and the energy storage system is being sized, an important consideration is given to what the cycling efficiency of the battery might be over the course of the expected mission duration. Section 3 addressed a number of the factors that determine the location of the different charging peaks and how they move either closer to or farther away from potentials where oxygen evolution causes the charging efficiencies to be reduced. Table 8 lists the milliampere hours of charge going into and out of 1-cm^2 pieces of electrode sample taken from plate no. 1. These results indicate that as the end-of-charge voltage is increased, the charge efficiency will be decreased due to the decreasing span between the charging curves and the point where oxygen evolution becomes excessive. Another important factor is the increase in capacity of electrode material, especially the well-cycled samples, when the cycling temperature is lowered. By using higher levels of cobalt additive in the active material, there will be an increase in the span between the voltage at which the active material is charged and the voltage where oxygen evolution becomes significant (Fig. 5). As a consequence of the data found in Fig. 4, a higher round-trip cycling efficiency should result with the use of 31% KOH as the electrolyte compared with 26% KOH. The advantage of 26% KOH over 31% KOH in certain applications appears to be due to smaller amounts of the material being converted to the gamma phase during the charge portion of the cycle. Excessive amounts of the lower density but higher capacity form of the charged material tend to cause the electrode to expand. In certain cells that have smaller amounts of electrolyte, this could result in cell dryout.

Table 8 documents the impact of temperature on the charge efficiency of samples taken from plate no. 1. The amount of charge into and out of each piece of electrode was obtained by integrating the areas under the charge and discharge portion of the EVS sweep of that sample. To consider how this relates to an actual cell, a typical 50-Ah nameplate cell will be used as an example. It might contain forty-eight 50-cm^2 electrodes in its plate pack. It would contain 2400 cm^2 of electrode. Assuming that an 86% round-trip efficiency is desired over a complete charge/discharge cycle, the cell would have a total capacity, including the residual capacity, of 98 Ah. A more typical capacity in an actual cell is closer to 60 Ah at the *C*/2 rate to a 1.2-V cut-off. This capacity does not include the low rate or residual capacity.

The FU data appearing in Table 4 also support the EVS data, showing that there is an increase in the usable capacity when charging for longer periods of time, which leads to a higher end-of-charge voltage. Also, there is more capacity available when cycling is carried out at lower temperatures. The high-rate (10 mA) capacity of a 48-plate cell when fully charged using material similar to that of plate no. 1 would be 94.53 Ah at room temperature and 98.74 Ah at −5 °C.

5. Impact of cycling conditions on cycle life

Two of the most important factors in determining the cycle life of cells, are the temperature at which they are cycled and the amount of overcharge that is put into the cell during the recharge portion of the cycle. The recharge ratio (RR) is very important in determining the ultimate cycle life of a cell or battery. there are several methods for selecting the RR to be used in a cycling test or a mission application. The ones that will be outlined here are based on the results of an extensive Aerospace review of the available data basing programs coupled with the relationships between charge

Table 8
Total capacities and charging efficiencies of 1.0-cm^2 pieces of electrode taken from the same good electrode and cycled to different end-of-charge voltages and different temperatures

End-of-charge EMF (V) vs. Hg/HgO	mAh charged at +10 °C	mAh discharge at +10 °C	Charge efficiency (%) at +10 °C	mAh discharge at −5 °C	Charge efficiency (%) at −5 °C
0.540	223.2	55.9	25.1	41.0	90.1
0.520	142.4	54.4	38.2	35.4	95.1
0.510	108.4	52.5	48.4	35.2	96.4
0.505	87.1	51.7	59.4	34.8	96.8
0.500	72.3	45.7	63.2		
0.495	55.7	44.5	79.9		
0.490	44.5	40.8	85.9		
0.485	40.8	36.9	92.0		
0.480	36.9	32.2	96.7		
0.470	22.1	21.7	98.3		

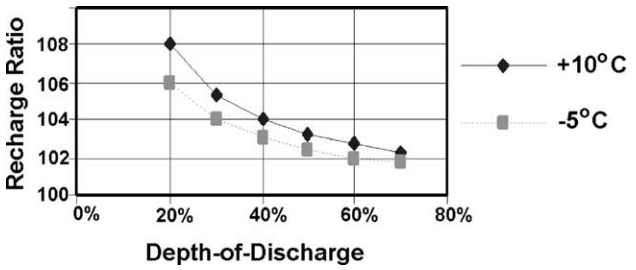

Fig. 7. Suggested safe recharge ratios based on reviewing cycling databases.

efficiency and state-of-charge [1]. The first method determines what might be called a "safe" RR. In this method, the results of previous long-term cycling studies were reviewed, and individual tests that displayed acceptable performance in terms of cycling duration and capacity maintenance during testing were noted along with their associated cycling temperature, RR, end-of-charge voltage, etc.

Cycling conditions have been examined that have resulted in long cycle lives (40,000 cycles at 40% DOD as an example), as evidenced by favorable amounts of remaining capacity and evidence of acceptable amounts of component degradation following the cycling test. The recharge ratios that were used in these tests were viewed as not being overly harmful to the integrity of the nickel electrodes. Based on the DOD, temperature, and RR used in each of these tests, the amount of overcharge in terms of ampere hours was calculated. For cycling conditions carried out at other DODs, this same amount of overcharge in terms of ampere hours should, as a first approximation, result in acceptable levels of damage to the cycling capabilities of the test articles. These are considered as "safe" levels of recharge. When this technique is applied to cells that have been tested at +10 °C and −5 °C, the following RRs, as shown in Fig. 7, are suggested for testing cells where extended periods of cycling are required.

A possible shortcoming of this method stems from the possible inconsistency between the DOD to which the cells are to be cycled and the SOC at which the cell desires to operate at the RR that is suggested by Fig. 7. If the cycling test used to select a safe level for the RR has allowed the cell to walkdown to 70% SOC when the cell charge protocol terminates the charge, then subsequent discharges beyond

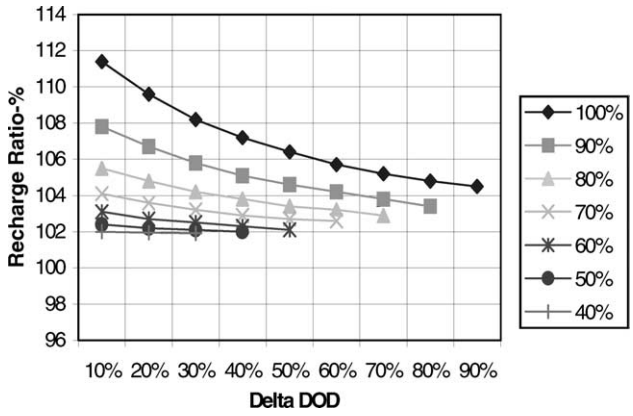

Fig. 9. Recharge ratio required to maintain the state-of-charge starting at different states-of-charge and discharging to different depths-of-discharge.

50% would not be recommended since the cell would be too close to being fully discharged at the end of a discharge cycle. Another possible shortcoming of this method is that, while it selects a safe recharge ratio, this RR may not be optimum level for cell performance.

A second method for selecting a RR determines what is called the "required" amount of recharge. This method is based on data that measures the charge efficiency as a function of the state-of-charge (SOC) of the cell design under study (Fig. 8). Unfortunately, this relationship is a function of temperature and cell manufacturer and it also changes as a cell is cycled. For this reason, the RR ratio to maintain a constant SOC changes with temperature, cobalt content of the active material, electrolyte concentration, DOD, and previous cycling history. This can be understood with the help of Fig. 8.

Fig. 8 is intended to illustrate the general relationship between the charge efficiency and SOC (relative to the nameplate capacity) at two different temperatures for a particular cell design when it is new [12]. As a cell approaches full charge, the charge efficiency decreases due to the increased amount of oxygen being generated in parallel with the charging reaction. Fig. 9 is generated using the relationship in Fig. 8 for the case of charging from 0 to 100% SOC at +10 °C. The top curve in Fig. 9, the one labeled 100%, is for a group of discharges that starts at 100% SOC based on the nameplate capacity. The point at 10% with

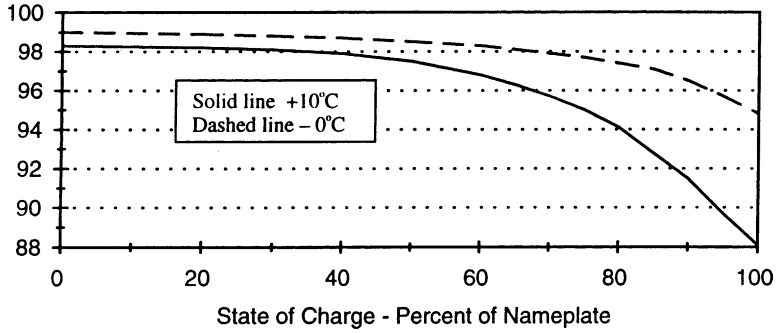

Fig. 8. Charge efficiency (%) as a function of state-of-charge for two different temperatures.

a corresponding RR of ∼111.4% means that a RR of ∼111.4% would be needed at +10 °C to cycle this cell when new from 100 to 90% SOC. If the cycle was to be from 100 to 80% SOC, the required RR would be 109.6%. If the cycling was to be from 90 to 50% SOC, the required RR would be 104.6%. It can be seen that as the cells are cycled to deeper DODs and the starting point is at lower and lower SOCs, smaller and smaller amounts of overcharge are required. It is for this reason that many of the Crane tests at 60% DOD may have experienced abbreviated cycling results. Often the same RR was used at both 60% DOD and 40% DOD. This resulted in excessive amounts of overcharge in the cells cycled to 60% DOD.

A possible difficulty with this second method is associated with extrapolating the RR into regions where the charge efficiency curve will suggest a certain amount of required overcharge that may be inconsistent with the amount of tolerable stress that can be safely applied to the cell. In the area where the safe RRs overlap the required RRs, long-term cycling results are to be expected while at the same time the usable capacity levels are maintained at the required levels.

6. Summary

An experimental program was carried out with the goal of gaining understanding related to the impact of certain cell design factors and cycling conditions on the ease by which nickel electrodes can be charged to different levels of usable capacity. Cell design factors including concentration level of KOH used as electrolyte and the amount of cobalt additive in the nickel hydroxide active material were found to impact the potentials at which the active material was charged first to the beta phase and then to the higher capacity gamma phase. The cycling temperature was found to be an important factor in selecting the cycling conditions since it resulted in a method to increase the separation in the potentials at which gamma phase formation occurred prior to the onset of excessive amounts of oxygen evolution. As the amount of oxygen evolution increases, the round-trip cycling efficiency decreases and the degradation rates are increased. Finally, two approaches were described for selecting an RR depending on whether long cycle life or high levels of usable capacity were desired. A full understanding of this topic is necessary in order to maximize the usefulness of the nickel–hydrogen system.

Acknowledgements

The help and cooperation of several individuals and organizations have been helpful in providing information that was used in the preparation of this report. The cycling data used in this report was made available from the life test sponsored by the Air Force and NASA. The test themselves were carried out at the Navy facility located at Crane, IN. Mr. Ralph James of the Air Force Research Laboratory in Albuquerque, NM, was instrumental in authorizing access to the day-to-day cycling data that was collected and stored at the Navy testing facility. Mr. Thomas Miller of the NASA Glenn Research Center in Cleveland, OH was helpful in facilitating access to the NASA-funded cycling database information that was also collected and stored at the Navy facility. Mr. Harry Brown, Mr. Bruce Moore, Mr. Stephen Wharton, and Mr. Jerry Davis of the staff at Crane were helpful in facilitating the sending of cells, cell components, and reports to Aerospace when they received authorization from the sponsoring agency. Destructive physical analysis studies made significant contributions to the conclusions and recommendations presented in this report. The laboratory procedures and techniques were carried out in our laboratories by Mr. Michael Quinzio. Dr. Margot Wasz examined many of the SEM specimens. The publications by other researchers interested in understanding the workings of the nickel electrode in nickel–hydrogen cells were helpful in developing our understanding of the very complicated electrochemical system.

References

[1] L.H. Thaller, A.H. Zimmerman, A Critical Review of Nickel–hydrogen Life Testing, Aerospace Report No. ATR-2001(8466)-2, May 2001.
[2] L.H. Thaller, A.H. Zimmerman, Optimum Recharge Protocols for Deep-Discharge Nickel–Hydrogen Cells and Batteries, Aerospace Report No. ATR-99(8466)-1, April 1999.
[3] L.H. Thaller, A.H. Zimmerman, G.A. To, Capacity Management and Walkdown During LEO Cycling of Nickel–Hydrogen Cells and Batteries, Aerospace Report No. TR-2001(3310)-1, October 2000.
[4] L.H. Thaller, Dealing with Capacity Loss Mechanisms in Nickel–Hydrogen Cells and Batteries, Aerospace Report No. ATR-2001(8466)-4, August 2001.
[5] R.D. Armstrong, G.W.D. Briggs, E.A. Charles, Some effects of the addition of cobalt to the nickel hydroxide electrode, J. Appl. Electrochem. 18 (1988) 215–219.
[6] K. Watanabe, M. Koseki, N. Kumagai, Effect of cobalt addition to nickel hydroxide as a positive material for rechargeable alkaline batteries, J. Power Sources 58 (1996) 23–28.
[7] J.D. Dunlop, G.M. Rao, T.Y. Yi, NASA Handbook for Nickel–Hydrogen Batteries, NASA Reference Publication 1314, 1993, pp. 5–21.
[8] R. Barnard, C.F. Randell, F.L. Tye, Studies concerning charged nickel hydroxide electrodes. I. Measurement of reversible potentials, J. Appl. Electrochem. 10 (1980) 109–125.
[9] S.U. Faulk, A.J. Salkind, Alkaline Storage Batteries, Wiley, New York, 1969, p. 533.
[10] L.H. Thaller, A.H. Zimmerman, G.A. To, Electrochemical Voltage Spectroscopy for Analysis of Nickel Electrodes, Aerospace Report No. TR-2000(8555)-3, January 2000.
[11] H.S. Lim, S.A. Verzwyvelt, Electrochemical behavior of heavily cycled nickel electrodes in nickel–hydrogen cells containing electrolytes of various KOH concentrations, in: Proceedings of the 16th International Power Sources Symposium, Bournemouth, UK, September 1988, pp. 341–355.
[12] A.H. Zimmerman, et al., Characterization and initial life-test data for computer designed nickel–hydrogen cells, in: Proceedings of the 1997 NASA Aerospace Battery Workshop, Huntsville, AL, 18–20 November 1997, pp. 471–484.